Islamic Azad University
Mashhad Branch

Dawod et al. / Iranian Journal of Earth Sciences 9 (2017) / 31-38

Pliocene volcanic activity of the Harrat Ash-Sham, South of Syria: geochemistry and petrogenesis

Safwan Dawod[*1], Ali Al-Mishwat[2], Abdulkarim Al Abdalla[3]

1. Ministry of Petroleum, the General Establishment of Geology, Syria
2. Department of Earth and Environmental Sciences, Kuwait University, Kuwait
3. Department of Geology, Tishreen University, Syria

Received 19 May 2016; accepted 4 December 2016

Abstract

The Cenozoic volcanic activity of the Harrat Ash Sham volcanic field in south of Syria is a part of the extensive magmatism that took place in the auxiliary extension faults along the Dead Sea Fault Zone from upper Eocene to Holocene. Pliocene volcanic rocks form an important part of igneous succession in Syrian Part of Harrat as Sham. These rocks vary from basalts flows to scoria. Pliocene basalts are divided into three primary petrographic groups: olivine basalt, olivine-pyroxene basalt and basanite. The three petro-types are alkaline and have similar compositional ranges of major and trace elements. Variations in the contents of major and minor elements in the Pliocene basaltic rocks are very slight. Such homogeneity in the chemical composition indicates to the operation of petrological processes that reinforced each other during the genesis of these rocks. The geochemical characteristics of the Pliocene basalt rocks reflect crystallization from primitive basic magmas that have experienced limited crystal fractionation process subsequent to their derivation by partial melting of the upper mantle.

Keywords: *Harrat Ash-Sham; Pliocene; Basalt; Volcanism*

1. Introduction

The northwestern part of the Arabian plate has experienced voluminous volcanic activity from Neogene to recent along the Dead Sea Fault Zone (DSFZ) (Bertrand et al. 2003; Shaw et al. 2003) (Fig. 1). Trifonov and Sokolov (2014) suggested that the beginning of a drift of the Arabia out of the African Plate and formation of the Dead Sea Transform occurred at ~20 - 17 Ma ago. Presently two periods of volcanism are recognized which are separated by this hiatus in the volcanic continuum in the Miocene-Pliocene time (Lustrino and Sharkov 2006). Sharkov et al. (1994) and Bilal (2009) concluded that the volcanism is presently active. Three separate volcanic complexes, Miocene, Pliocene and Quaternary, represent the volcanic rocks of Syrian part of Harrat Ash-Sham region. The volcanic activity during the Pliocene time starts with a fissures volcanism (Sharkov et al. 1994) exposure mostly as NNW-trending (Bilal and Sheleh 2004). Large basaltic lava flow exposure cover an area of several hundred square kilometers area, extending to the Alhara desert in the east of Harrat Ash-Sham and to the northeastern part of Jordan (Yaseen 2014).

In spite of the volcanic activity in the Harrat Ash-Sham is extend from the middle Mesozoic to recent time (Shaw et al. 2003), the Pliocene volcanism was the most important stage because the volcanic activity in this period accompanied with a large earthquakes (Florentin et al. 2014) and development the uplift with mainly left lateral strike slip that took place on the Dead Sea fault zone (Chorowicz et al. 2005) in a complex geodynamics setting (Lustrino and sharkov 2006). On the other hand, the geochemical characteristics of the Pliocene basalt flows are various and imply many indications about the origin of these rocks. Therefore this study focuses on petrographic, geochemical and petrogenesis sides to answer of several points related to the basalt that erupted during the Pliocene age in southern of Syria.

---

*Corresponding author.
E-mail address (es): safwandawod@yahoo.com

2. Regional Geology

The Harrat Ash-Sham volcanic field is the largest volcanic field on the Arabian plate. It extends from the southern edge of Damascus basin in Syria to east of Wadi Sirhan Depression in Saudi Arabia (Fig 1). The Syrian part of the Harrat Ash-Sham volcanic field contains several hundred volcanic centers (Ponikarov et al. 1966) which imply pyroclastic cones, shield volcanoes and composite volcanoes settled down along northwest-trending faults that bound asymmetric grabens. Opening and rifting motion of the DSFZ formed a strike–slip fault system with both creeps (Doglioni et al. 2015) extending from the Red Sea in the south to the East Anatolian Fault Zone in the north (Westaway et al. 2008; Karabacak et al. 2010).This motion influenced the region from southwest Jordan to

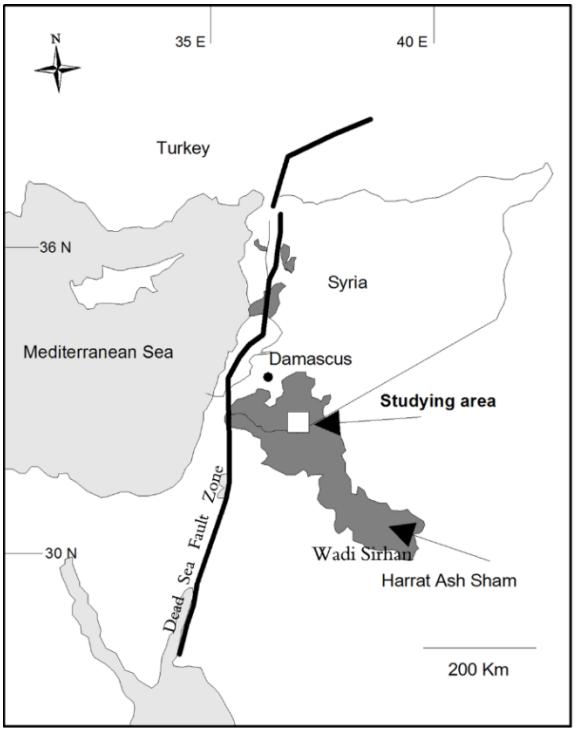

Fig 1. simplify map show the Harrat Ash Sham Volcanic Field and position of the studying area.

southern Turkey and caused a significant tectonic reorganization and concomitant volcanic activity (Giannérini et al. 1988; Alpaslan 2007). Olivine basalt and basanite form a full part of the global basaltic inventory in Harrat Ash-Sham region volcanic field (Ponicarov et al. 1966; Lustrino and Wilson 2007). It comprises a part in the easternmost realm of the encompassing Circum-Mediterranean Anorogenic Cenozoic Igneous province (CiMACI) described by Lustrino and Wilson (2007).

3. Local Geology

Basaltic Pliocene flows in southern of Syria that broadly similar in the field, extend to several hundred kilometers square (Fig 2a). As some early Pleistocene volcanos, Basaltic Pliocene emerges from extension faults or central cones coincide or follow the development of the Dead Sea fault zone. Volcanic Pliocene flows are exposed as eroded, massive rocks and represented by numerous alternations of lava sheets, often separated by horizons of red clays. The thickness of sheet ranges from 2 to 16m. In the field, these sheets have similar morphological features. The upper and lower of each pants of these are composed of vesiculated basalt, while the central part is composed of well crystallized massive varieties. A variety of volcanic features are shown by these rocks in the field especially in the exposures of Mshannaf area (Fig 2b). The external volcanic forms of these rocks are the most obvious field feature which can be used to distinguish among the different types of the Pliocene volcanic exposures. Such forms include columnar joints and internal parting surfaces within individual massive flows. These partings produce thin slabs which are 10 to 20 cm thick but may reach 50 cm. Flow surfaces are fragmented, with the fragmentation extending downward into the flow body, a feature which may indicate a prolonged period of subaerial exposure (Single and Jerram 2004), and are associated with volcaniclastic tuff. Lava flows terminate by bifurcating into minor lobs which inter-finger with thin colluviums.

Xenoliths accompanying the Pliocene volcanic field found in extensive basalt flows forming cores of volcanic bombs and other pyroclastic forms and tuffaceous materials. Most xenoliths are irregularly, but also elongated and range from 8 cm to 24 cm in diameter.

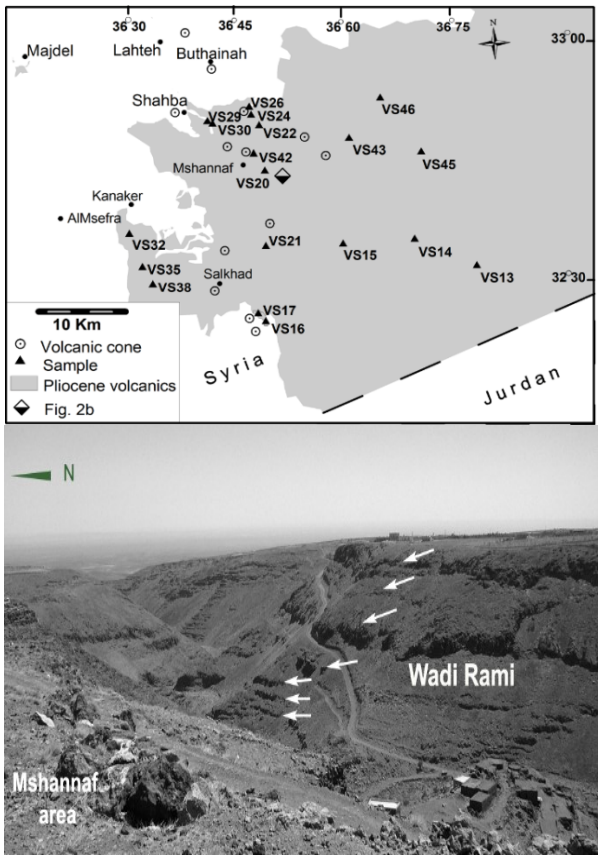

Fig 2. (a) Geological map of the Pliocene Volcanic Field in South of Syria showing site of the studying samples. (b) The Pliocene section of Wadi Rami, Mshannaf area. Note the basaltic flows that represented by numerous alternations of lava sheets (white arrow). Location of photo: N°32.753574, E°36.799553.

4. Analytical Methods

Twenty fresh basaltic samples were collected from the Pliocene volcanic field for the purpose of performing geochemical analysis. Thin sections were prepared for petrographic study in the Department of Earth and Environmental Sciences, Kuwait University.

Representative powdered rock samples were used for geochemical analyses of samples that minimal alteration. Geochemical analyses of samples were determined using a fully computer-controlled SIEMENS SRS3000 sequential wavelength XRF spectrometer equipped with a Rhodium target tube. Proprietary SPECTRA4 software was used for running the spectrometer and managing the data calculation and reduction. An ensemble of well-analyzed and internationally-certified natural rock standards was utilized for establishing the calibration curves for elements. Major elements oxide compositions were determined on glass disks. Five grams of rock sample powder was fluxed with ten grams of flux prepared by thorough mixing of Lithiumtetraborate (80%) and Lithium metaborate (20%). Under the supervision of the Department of Earth and Environmental Sciences, Kuwait University, minor elements were determined on pressed powder pellets. Loss on ignition (LOI) was determined on rock powders ignited at 1100°C. Concentrations of elements were corrected for the weight loss and oxidation.

5. Petrography

The Pliocene rocks in south of Syria are dominated volumetrically by three lithologies, olivine basalt, olivine-pyroxene basalt and basanite.

5.1. Olivine basalt

Olivine basalt is the dominant basaltic variety petrographic rocks type in the study area. Olivine phenocrysts are euhedral to subhedral spread in the ophitic texture and forms 6 to 17% of the rock (Table 1) with diameters of up to 2.5 mm. Olivine phenocrysts often surrounded by alteration rim (Iddingsitisation). Clinopyroxene forms subhedral phenocrysts. It often forms a glomorphical structure with olivine's phenocrysts. Opaque minerals form an important ratio of the rock (~ 4 to 7%) accompanied with hexagonal feature of Apatite which sets in a groundmass of microcrystalline matrix of plagioclase and olivine and pyroxene with a relatively high ratio of glass and zeolite as seen in some comparable area like Jabal Huliat in Jordan (Al Dwairi and Sharadqah 2014).

5.2. Olivine-pyroxene basalt

Olivine-pyroxene basalt is porphyritic rocks with holocrystaline to microlites groundmass. Plagioclase is commonly euhedral to subhedral or occurs as small-microliths within the groundmass. It rarely shows oscillatory zoning and sericite alteration. Olivine phenocrysts are second dominant mineral phase. It is euhedral to subhedral in shape and form 8 to 15% of the rock (Table 1). The clinopyroxene (8-18%) are subhedral phenocrysts with two cleavages and sometime exhibit zoning, and lamellar twinning. Augite is the dominant pyroxene's mineral and subordinate aegrine augite. Pyroxene occurs in the microcrystalline matrix or together with olivine and plagioclase as poicklitic texture. In some samples pyroxene crystals contain magnetite. Glass constitutes about 8 to 23% of the groundmass.

Table 1. Modal compositions (volume %) of the main minerals in the Pliocene basalt from south of Syria.

Basanite	Olivine-pyroxene basalt	Olivine basalt	
15-20 %	8-15 %	6-17%	Olivine
6-10 %	8-18 %	6-9 %	Clinopyroxene
7-18 %	8-21 %	9-22 %	Plagioclase
2-3 %	2-4 %	3-4 %	Alkali feldspar
2-4 %	2-4 %	2-4 %	Magnetite
2-3 %	2-4 %	2-3 %	Ilmenite
3-8 %	8-23 %	4-10 %	Glass

5.3. Basanite

Basanite occurs as dark colored and forms massive flows that occasionally contain vesicles. The basanite samples are fine grained, hypocrystalline and show porphyritic textures. Most common phenocrysts are olivine, which is generally euhedral to subhedral and usually is dominant, forming up 15 to 20% of the rock (Table 1). Augite is mostly subhedral and pale pink to purple in plane polarized light. Fine-grained clinopyroxene measures about 0.1 millimeter and is situated between opaque minerals or set as mesostasis in a groundmass. Albite phenocrysts and acicular laths are partly replaced by sericite.

6. Geochmistry

On the total alkali-silica (TAS) classification diagram of Le Bas et al. (1986) all analyzed rocks fall in the alkaline field (Fig. 3). The diagram reveals that the most samples can be classified as basalt and basanite, but two samples plot in the trachy-basalt field.

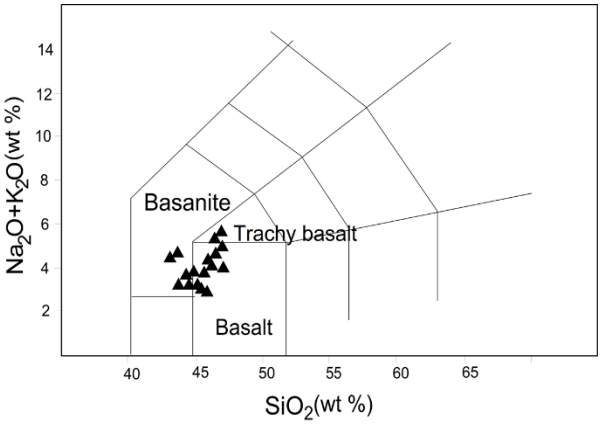

Fig (3): Total alkali versus silica (TAS) diagrams for chemical classification of the Pliocene samples. After (Le Bas et al., 1986).

The SiO_2 content varies in a restricted range from 43.07 wt% to 47.2 wt%. MgO also shows a somewhat mild

variation from 4.3 wt% to 11.55 wt%. The K2O content varies in the investigated rocks from 0.61 wt% to 1.86 wt%, while the Na_2O content varies from 2.35 wt% to 3.85 wt%. The Al_2O_3 content show is relatively high (with average about 15.83%). It distributed between plagioclase and feldspar minerals that prevalent in the studying rocks. Fe_2O_3+FeO shows similarity content in most samples that variety are about 9.87 to 18.96 with Fe_2O_3 value higher than FeO value. FeO considers multiphase oxide that is appear in magnetite and iliminite minerals and as patches of magnetite on corroded olivine, while Fe_2O_3 often linked to alteration process of iddingsite.

The most common minor incompatible elements concentration ratios for the studied samples are lists in Table 2. The investigated rocks are characterized by their high concentration of compatible elements including Co, Ni, Cr, Cu and V. Barium varies from 637 to 713 ppm and 653 to 911 ppm for strontium.

Table 2. Content of major elements oxides (wt %) and trace elements (ppm) of basaltic rock samples from south of Syria. na: not analysis.

Sample	SiO_2	TiO_2	Al_2O_3	Fe_2O_3	FeO	MgO	CaO	Na_2O	K_2O	Co	Cr	Ni	Ba	Sr	V	Zr	Nb	D.I.	Mg#
VS13	43.66	1.99	14.59	4.96	9.91	10.51	9.74	3.7	0.95	65	297	161	661	854	182	215	74	27.27	63.8
VS14	44.58	1.88	17.63	5.19	10.38	5.54	11.56	2.39	0.85	47	294	121	712	822	171	234	92	23.54	77.79
VS15	45.98	1.84	16.31	5.15	10.31	6.39	9.59	3.32	1.09	30	331	122	658	742	170	241	90	31.35	75.11
VS16	46.44	2.46	14.98	4.87	9.44	6.24	10.11	3.71	1.66	44	222	143	712	687	178	212	82	34.61	74.1
VS17	44.17	3.67	13.5	4.55	9.08	10.63	10.61	3.01	0.71	50	218	162	771	801	188	195	72	24.78	61.5
VS20	44.68	2.31	10.64	6.09	12.87	10.45	9.04	2.62	0.95	47	234	140	607	653	182	224	95	26.34	69.36
VS21	45.91	2.04	16.49	5.71	5.33	10.88	10.56	2.35	0.66	41	250	114	623	643	180	231	91	23.78	55.4
VS22	45.54	1.24	17.98	4.07	8.2	8.02	11.4	2.56	0.61	71	252	167	646	622	177	233	84	23.22	65.6
VS24	47.2	1.45	19.71	4.44	8.8	4.3	9.87	3.16	0.93	67	209	101	611	812	171	244	87	32.14	79.32
VS26	46.88	2.46	16.84	4.19	8.35	5.55	10.44	3.6	1.32	na	na	na	na	na	na	na	na	33.66	73.79
VS29	43.62	2.24	14.32	5.46	10.36	11.55	8.89	2.36	0.86	73	256	164	786	911	193	255	117	24.68	64.5
VS30	44.56	2.31	13.18	5.37	13.3	8.05	8.07	2.89	1.02	49	222	155	683	949	184	212	77	29.52	74.4
VS32	44.64	2.18	15.12	4.31	8.64	10.63	10.54	3.01	0.75	70	206	160	617	935	186	257	106	24.56	61.3
VS35	46.22	1.12	15.13	3.8	7.48	10.66	11.24	3.19	0.82	na	na	na	na	na	na	na	na	25.71	57.9
VS38	45.04	1.4	17.45	4.37	8.79	8.76	10.06	2.7	0.69	na	na	na	na	na	na	na	na	24.98	67.2
VS42	44.57	1.72	16.56	4.26	9.02	7.88	12.42	2.51	0.8	na	na	na	na	na	na	na	na	21.31	67.8
VS43	46.32	2.57	17.74	4.42	8.84	6.88	8.58	3.8	0.85	32	157	125	697	951	187	228	79	34.21	70.6
VS44	46.79	1.83	19.97	3.32	6.55	5.85	9.18	3.85	1.86	na	na	na	na	na	na	na	na	36.88	67.7
VS45	43.07	3.11	11.69	5.52	11.05	10.54	10.51	3.04	1.47	72	248	164	783	769	180	234	85	25.51	66.2
VS46	45.57	2.74	16.79	4.79	9.58	6.05	10.51	2.95	0.94	40	213	133	636	639	198	204	74	28.63	74.74

Oxides (wt %), trace (ppm).
D.I.: differentiations index, Mg#: (magnesium number) = MgO/(MgO + FeOtot)

7. Discussion

Variations in the contents of major and minor elements in the Pliocene basaltic rocks are very slight. Such homogeneity in the chemical composition reflects the operation of petrological processes that reinforced each other during the genesis of these rocks.

7.1. Fractionation- differentiation

Harker variation diagrams (Fig. 4) display the variations in the major oxides and most common trace elements plotted against the silica content. The variation trends are explained by fractionation of mineral phases observed in the rocks. For example, the decrease in the FeO and Fe_2O_3 contents, against an increase of silica (Fig. 4) is explained by fractionation of mafic minerals. The decrease in the MgO content with silica can be explained by the fractionation of olivine and clinopyroxene, and may explain also the unclear decrease of CaO, Ba and Sr (Wilson 1989; Eby et al. 1998). Depletion in Ba and Sr in the studied rocks (Fig. 4) can be attributed to the fractionation of alkali feldspar and plagioclase. The relatively narrow range of MgO and low values of the differentiations index (D.I.) (21.31-36.88, averaging 27.8) and the magnesium number (ave. 68.41) (Table. 2) together with clustering of Ni and Co (Shaw et al. 2003; Krienitz et al. 2007) and Al_2O_3 vs. MgO correlation (Wilson 1989) (Fig. 5) are features viewed as evidence for insignificant or lack of fractionation and differentiation.

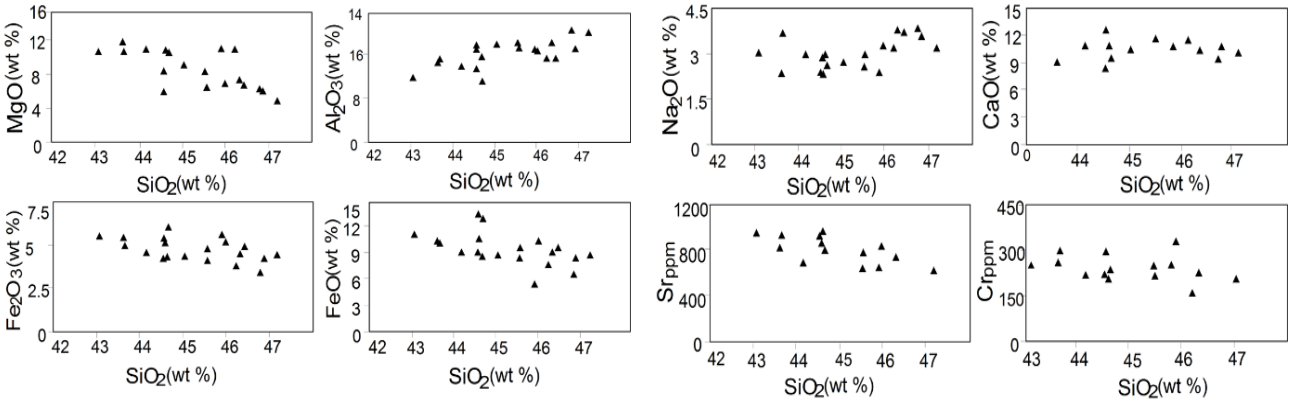

Fig (4): Harker variation diagrams for the Pliocene samples from south of Syria.

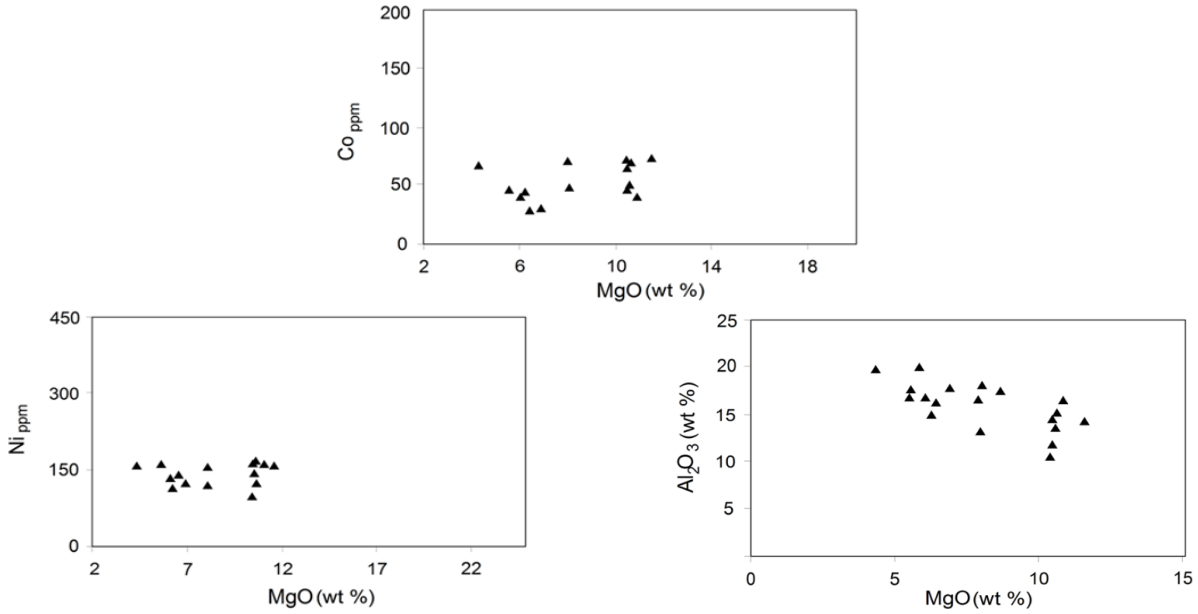

Fig (5): a) Ni versus MgO diagram after (Achepkov, 1991). b) Al_2O_3 versus MgO diagram.

Irvine (1965) showed that chrome-spinel, the main repository of Cr, crystallizes at an early stage of solidification of primary magmas. High concentration of Cr in the earliest crystallization product in primary mafic magmas can be explained by early coupled separation of chrome-spinel (or Cr in solid solution in magnetite) and clinopyroxene (Bell et al. 1994). The slight negative correlation of Cr with silica (Fig. 4) is attributed to the fractionation of clinopyroxene and minor quantities of Cr-spinel from the initial magma, an interpretation similar to that of Preston et al. (1998). The high content of Cr (240.6 ppm) in the studied rocks is much higher than the value of 142 ppm tabulated by Hughes (1982) for primary basaltic magma. This high Cr content in the investigated rocks is inconsistent with the Pliocene magmas having undergone any significant differentiation or crystal accumulation processes.

The relatively high abundances of Cr and Ni in the Pliocene volcanic field in Syrian part of Harrat Ash-Sham region attest to a very small change in the magma since its formation, an explanation which had been reached for neighbor Harrat Al Fahda area in Jordan by Ibrahim and Al-Malabeh (2006).

Another illustration pertaining to this lack of signs for significant differentiation-fractionation is the relationship between each of the ratios of Ni/FeO and Co/FeO and Al_2O_3/MgO ratio (Fig. 6).

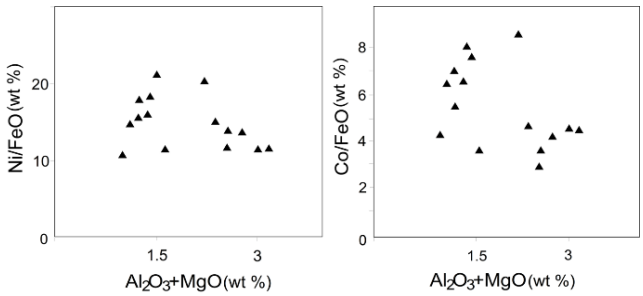

Fig (6): Al_2O_3/MgO versus Ni/FeO and Co/FeO diagrams on condition that MgO > 3 wt %. After (Francalanci et al., 2000).

Francalanci et al. (2000) used similar plots to assess the degree of differentiation-fractionation and concluded

that only clearly unambiguous relationships in them can be utilized as evidence of fractionation. The lack of significant differentiation-fractionation signs may be attributed to a rapid rise of the magmas through the upper mantle and the crust.

7.2. Magma mixing and partial melting

The extent of magma mixing has a direct influence on chemical variations in magmas while moving upward through the upper mantle and crust (Francis and Ludden 1990). Magma mixing requires simultaneous coexistence of more than one magma with contrasting chemical compositions (Sigmarsson et al. 1998; Thomas et al. 1999). The magma mixing processes are represented by mixing lines in plots like that relating Zr and Nb abundances (Reiners and Nelson 1998) in the Zr-Nb variation space. These two elements generally produce a linear trend of variation, similar to that in Fig 7.

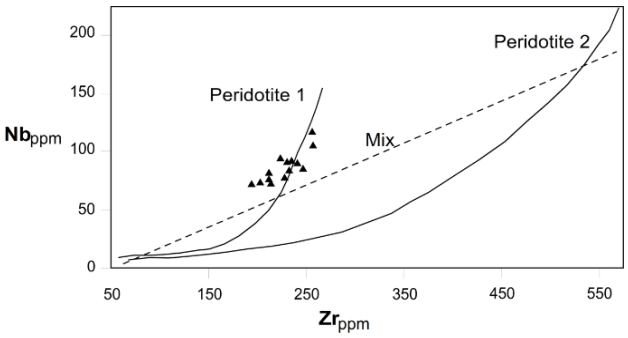

Fig (7). Zr versus Nb diagram for modeling partial melting of peridotite (Reiners 2002) and the line of trend of mixing. After Sigmarsson et al., (1998) and Thomas et al., (1999).

This plot of the Zr-Nb co-variations for the investigated rocks illustrates their concomitant co-variation falls far from the mixing line. This divergence signifies the improbability of magma mixing as a viable participating mechanism during the genesis of the Pliocene basalts in south of Syria.

The partial melting process which is responsible for the generation of basaltic melts can be analyzed with the aid of the Zr-Nb plot in Fig. 7, which shows a summary of partial melting of three different pyrolite models containing peridotite assemblages with contrasting contents of olivine, clinopyroxene, orthopyroxene and garnet (Reiners 2002). This figure show, in addition to the magma mixing line described above, the Zr-Nb plots for the three pyrolite would lead to production of basaltic liquids. Each of these models is represented by a unique and discrete curve that predicts the behavior of these two elements during melting. Regardless of the composition of the ultramafic mantle source rocks, each model predicts curved trends for the Nb and Zr changes. The Zr-Nb variations for the studied rocks adhere very closely and are in a good agreement with the curve displaying partial melting of model peridotite 1.

8. Conclusion

An extensive volcanic activity developed from Miocene to Holocene in the northernmost part of the Harrat Ash Sham volcanic field within Syria. The Pliocene volcanic rocks in this area constitute an important component of the mafic products which occur in different forms: continuous lava flows, cinder cones and tufaceous sheet deposits. A series of interfaces components types have been define in the lava flow structure.

The studied rocks are mainly composed of olivine, plagioclase, and augite phenocrysts enclosed by fine- to medium-grained. Modally, three essential petro-types are recognized including: olivine basalt, olivine pyroxene basalt and Basanite. Petrochemical classification indicates that the two essential petro-types can be classified as alkali basalt and basanite with similar compositional ranges of major and trace elements. Several preliminary conclusions derived regarding the petrological and geochemical characters of the investigated volcanic rocks which indicate that the Pliocene basaltic melts had generated by partial melting process. The relatively homogenous chemical composition of the Pliocene basalts can be explained by the magmas having limited fractionation process.

Acknowledgment

The authors are grateful to Dr. Ahmad Bilal from Damascus University for useful tectonic discussions. We are also grateful to the staff of the General Research Facilities (GRF) in the College of Science in Kuwait University for providing the XRF geochemical analyses.

References

Al Dwairi R, Sharadqah S (2014) Mineralogy, Geochemistry and Volcanology of Volcanic Tuff Rocks from Jabal Huliat Al-Gran, South of Jordan. *Jordan Journal of Civil Engineering* 8:188.

Alpaslan M, (2007) Early to middle Miocene intra-continental basaltic volcanism in the northern part of the Arabian plate, SE Anatolia, Turkey. *geochemistry and petrogenesis. Geological magazine* 144:867-882.

Bell B.R, Clayton R.V, Rogers G, (1994) The petrology and geochemistry of cone-sheets from the Cuillin igneous complex, Isle of Skye: evidence for combined assimilation and fractional crystallization during lithospheric extension. *Journal of Petrology* 35:1055–1094.

Bertrand H, Chazot G, Blichert-Toft J, Thoral S (2003) Implications of widespread high-K volcanism on the Arabian Plate: implications for the Afar mantle plume and lithosphere composition. *Chemical Geology* 198:47–61.

Bilal A, Sheleh F (2004) Un "point chaud" sous le systeme du Rift syrien: donnees perologiques complementaires sur les enclaves du volcanisme recent. *Comptes Rendus geoscience, Paris* 336:197-204.

Bilal A (2009) Seismicity and volcanism in the rifted zone of western Syria. *Comptes Rendus Geosciences* 341:299-305.

Chorowicz J, Dhont D, Ammar O, Rukieh M, Bilal A (2005) Tectonics of the Pliocene Homs basalts (Syria) and implications for the Dead Sea Fault Zone activity. *Journal of the Geological Society, London* 259-271.

Doglioni C, Barba S, Carminati E, Riguzzi F (2015) Fault on-off versus strain rate and earthquakes energy. *Geoscience Frontiers* 6:265-276.

Eby G.N, Woolley A.R, Din V, Platt G (1998) Geochemistry and Petrogenesis of Nepheline Syenites: Kasungu-Chipala, Ilomba, and Ulindi Nepheline Syenite Intrusions, North Nyasa Alkaline Province, Malawi. *Journal of Petrology* 13:1405-1424.

Florentin J, Blackwell B, Tüysüz O, Tarı U, Genç S, İmren C, Mo S, Huang Y, Blickstein J, Skinner A, Kim M (2014) Monitoring tectonic uplift and paleoenvironmental reconstruction for marine terraces near MAĞARACIK and SAMANDAĞ, Hatay province, Turkey. *Oxford University Press, Radiation Protection Dosimetry* 160:Abstract.

Francalanci L, Innocenti F, Manetti P, SavascËin Y (2000) Neogene alkaline volcanism of the Afyon-Isparta area, Turkey: petrogenesis and geodynamic implications. *Mineralogy and Petrology* 70:285-312.

Francis D, Ludden J (1990) alkaline olivine basalt at Fort Selkirk, Yukon, Canada. *Journal of Petrology* 31:371–400.

Giannérini G, Campredon R, Feraud G, Abo Zakhem B (1988) Déformations intraplaques et volcanisme associé: exemple de la plaque arabique au Cénozoïque. *Bullton Society of Géology* 6:937-947.

Hughes C (1982) Igneous Petrology. Development in Petrology. Elsevier, New York. 53p.

Ibrahim K.M, Al-Malabeh A (2006) Geochemistry and volcanic features of Harrat El Fahda: a young volcanic field in northwest Arabia, Jordan. *Journal of Asian Earth Sciences* 27:147-154.

Irvine T.N (1965) Chromian spinel as a petrogenetic indicator: Part 1. Theory. *Canadian Journal of Earth Science* 2:648-672.

Karabacak V, Altunel E, Meghraoui M, Akyüz H.S (2010) Field evidences from northern Dead Sea Fault Zone (South Turkey): New findings for the initiation age and slip rate. *Tectonophysics* 480:172-182.

Krienit M, Haase K, Mezger K, Shaikh-Mashail M. A (2007) Magma Genesis and Mantle Dynamics at the Harrat Ash Shamah Volcanic Field (Southern Syria). *Journal of Petrology* 48:1513-1542.

Le Bas M.J, Le Maitre R.W, Streckeisen A, Zanettin B (1986) A classification of volcanic rocks based on the total alcalis-silica diagram. *Journal of Petrology* 27:745-750.

Lustrino M, and Sharkov E.V (2006) Neogene volcanic activity of western Syria and its relationship with Arabian plate kinematics. *Journal of Geodynamics* 42:115-139.

Lustrino M, Wilson M (2007) The circum-Mediterranean anorogenic Cenozoic igneous province". *Earth-Science Reviews* 81:1-65.

Ponikarov V.P, Kazmin V.G, Mikhailov I.A, Razvaliayev A.V, Krasheninniko, V.A, Kozlov V.V, Soulidi-Kondratiyev E.D, Faradzhev V.A (1966) In The geological map of Syria, scale 1:1,000,000: explanatory notes" Vsesoj. Exportno-Import Objed. Technoexport, Moscow, and Ministry of Industry, Syrian Arab Republic, Damascus.

Preston R.R, Bell J. B, Rogers G (1998) The Loch Scaridain xenolithic Sill Complex, Isle of Mull, Scotland: fractional crystallization, assimilation, magma-mixing and crustal anatexis in subvolcanic conduits. *Journal of Petrology* 39:519 –550.

Reiners P.W, Nelson B.K (1998) Temporal-compositional-isotopic trends in rejuvenated-stage magmas of Kaua'i, Hawaii, and implications for mantle melting processes. *Geochimica Cosmochimica Acta* 62:2347–2368.

Reiners P.W (2002) Temporal-compositional trends in intraplate basalt eruptions: Implications for mantle heterogeneity and melting processes. *Geochemistry, Geophysics, Geosystems* 3:1525-2027.

Shaw J.E, Baker J.A, Menzies M.A, Thirlwall M.F, Ibrahim K.M (2003) Petrogenesis of the largest intraplate volcanic field on the Arabian Plate (Jordan): a mixed lithosphere–asthenosphere source activated by lithospheric extension. *Journal of Petrology* 44:1657–1679.

Sharkov E.V, Chernyshev I.V, Devyatkin E.V, Dodonov A.E, Ivanenko V.V, Karpenko M.I, Leonov Y.G, Novikov V.M, Hanna S, and Khatib K (1994) Geochronology of Late Cenozoic basalts in Western Syria. *Journal of Petrology* 2:385–394.

Sigmarsson O, Carn S, Carracedo J.C (1998) Systematics of U-series nuclides in primitive lavas from the 1730- 36 eruption on Lanzarote, Canary Islands, and implications for the role of garnet pyroxenites during oceanic basalt formations. *Earth and Planetary Science Letters* 162:137–151.

Single R.T, Jeram D.A (2004) The 3D facies architecture of flood basalt provinces and internal heterogeneity: examples from the palaeogene Skye Lava Field. *Journal of geological society, London* 161:911-926.

Thomas L.E, Hawkesworth C.J, Van Calsteren P, Turner S.P, Rogers N.W (1999) "Melt generation beneath ocean islands: A U-Th-Ta isotope study from Lanzarote in the Canary Islands. *Geochimica Cosmochimica Acta* 63:4081 – 4099.

Trifonov V, Sokolov S (2014) Late Cenozoic Tectonic Uplift Producing Mountain Building in Comparison with Mantle Structure in the Alpine-Himalayan Belt. *International Journal of Geosciences* 5:26.

Westaway R, Demir T, Seyrek A (2008) Geometry of the Turkey-Arabia and Africa-Arabia plate boundaries in the latest Miocene to Mid-Pliocene: the role of the

Malatya-Ovacık Fault Zone in eastern Turkey. *eEarth* 3:27–35.
Wilson M (1989) Igneous Petrogenesis, Unwin-Hyman, London, 46 p.
Yaseen I (2014) Petrography and Mineral Chemistry of the Almanden Garnet, and Implication for Kelyphite Texture in the Miocene Alkaline Basaltic Rocks North East Jordan. *International Journal of Geosciences* 5:36.